NUMERICAL INVESTIGATION OF INTERFERENCE FIT ASSEMBLIES AND THE INFLUENCE OF VARYING THE LAMINATE THICKNESS

P. Fahr[1] and R. Hinterhölzl[1]

[1]Institute for Carbon Composites, Faculty of Mechanical Engineering, Technische Universität München, Boltzmannstraße 15, D-85748 Garching b. München, Germany
Email: fahr@lcc.mw.tum.de, Web Page: http://www.lcc.mw.tum.de
Email: hinterhoelzl@lcc.mw.tum.de

Keywords: Interference Fit Assembly, Composites, Thick-Walled, Numerical Analysis, Hybrid Joints

Abstract
For hybrid joints between CFRP drive shafts and metallic hubs the interference fit assembly (IFA) is a fibre suitable joining technique. To improve the analysis with an easy applicable analytical approach and give design recommendations both for thick-walled IFAs the influence of several mechanical and tribological phenomena as well as several design parameters need to be investigated. In a former study the assembly process has been investigated experimentally and the test specimens have been analysed with an analytical approach. In this study these test specimens are analysed with a rotationally symmetric numerical linear elastic model. The results are compared to the experimental and analytical values. The influence of the laminate's thickness on the contact pressure is numerically investigated within a parameter study.
The numerical values deviate less from the experimental results than the analytical values. This deviation shows no dependency from the thickness of the parts. Increasing the outer 90°-layers' thickness influences the contact pressure less the thicker the parts are. A critical 90°-layers' thickness is determined, for which the contact pressure is almost constant for a varying thickness of the inner layers. The critical thickness depends on the angle of the balanced laminate and can be scaled with the corresponding scaling factor for scaled parts.

1. Introduction

To reduce the energy consumption of mechanical systems by reducing weight and inertia of accelerated parts the need for lightweight structures is increasing. Fibre reinforced plastics (FRPs) perfectly suit these lightweight applications due to their outstanding specific stiffness and strength properties. For drive shafts the eigenfrequencies can be increased especially by the application of carbon fibre reinforced plastics (CFRPs). Therefor a bisection of long shafts and additional bearings can get unnecessary, thus enabling secondary weight savings. Load introductions often result in stress concentrations and therefor are critical areas in a structure. Parts made of FRP are often joined with other materials. These hybrid joints make further demands on the joining technique. The interference fit assembly (IFA) between an inner steel hub and an outer CFRP shaft is a fibre suitable, cost-efficient and easy to realise joining technique for shafts. To facilitate the use of CFRP computationally economic and easily applicable ways of analysing composite parts and joints are needed. Analytical approaches do not make costly and computationally intensive commercial numerical tools necessary. But their applicability and accuracy is often limited by fundamental assumptions for the mechanical behaviour of the parts. A current analytical approach for finite orthotropic IFAs is presented in [1]. For thick-walled parts the accuracy of this approach is limited, which was shown in [2]. To develop the analytical analysis, parameters and phenomena influencing the IFA and its analysis must be

Excerpt from ISBN 978-3-00-053387-7

investigated. The knowledge concerning these effects must be broadened and dependencies must be pointed out to identify relevant effects and consider them in the analytical analysis.

In [2] the assembly process of IFAs by force fitting is investigated experimentally. Steel hubs are inserted with interference into CFRP shafts at room temperature. The CFRP shafts consist of inner ±30°-layers with thickness $t_{\pm 30°}$ and outer 90°-layers with thickness $t_{90°}$ (see Figure 1). The angle of the layers is measured at the axis of the shaft. More information concerning manufacturing and material of the parts is given in [2].

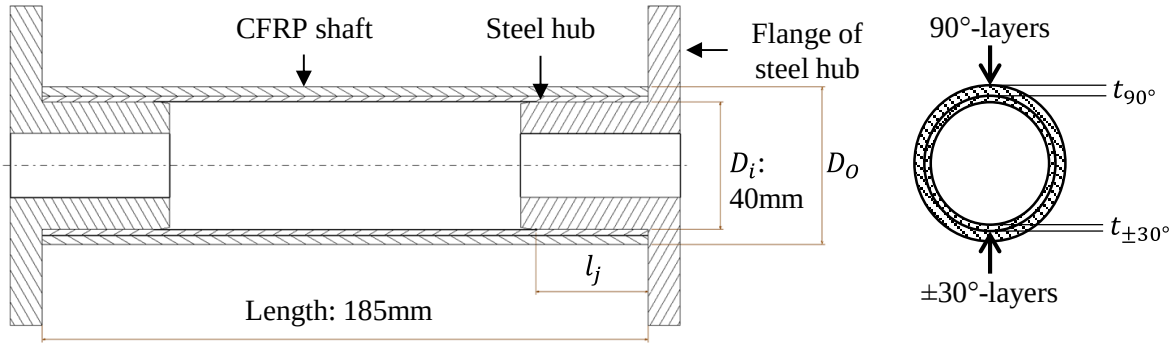

Figure 1. General composition of the test specimens (left side); laminate layup of the test specimens (right side) [2]

The thicknesses $t_{\pm 30°}$ and $t_{90°}$ of the layers, the roughness R_z of the steel hubs, the interference In between the parts and the length l_j of the joint are varied within the experimental layout (see Table 1).

Table 1. Parameters, ratio of diameters and tested amount of specimens for the combinations [2]

Combination	$t_{\pm 30°}$ [mm]	$t_{90°}$ [mm]	R_z [µm]	In [mm]	l_j [mm]	R_{Oi} [-]	N [-]
Reference	1.8	5.6	8	0.075	35	1.37	3
±30° thick	7.2	5.6	8	0.075	35	1.64	8
90° thick	1.8	11.2	8	0.075	35	1.65	4
Rough	1.8	5.6	16	0.075	35	1.37	3
Large interference	1.8	5.6	8	0.125	35	1.37	3
Short joint length	1.8	5.6	8	0.075	17.5	1.37	3

The specimens are characterized concerning geometry and material parameters. During the assembly the applied axial force is measured by a load cell and the tangential strain on the outer surface of the CFRP shaft is measured by a digital image correlation system. From this data the assembly force $F_{a,exp.}$ and the tangential strain $\varepsilon_{\theta,r_A,exp.}$ in the middle of the joint are determined (see [2]). The results of the experiments show that increasing R_z reduces $F_{a,exp.}$ and $\varepsilon_{\theta,r_A,exp.}$. Increasing $t_{90°}$ less than proportionally increases $F_{a,exp.}$ and increasing $t_{\pm 30°}$ decreases $F_{a,exp.}$.

The specimens have been analysed with the analytical approach from [1], in which the following assumptions are made. Parts are considered to be thin-walled and radial stresses are neglected. The material behaviour is linear elastic and deformations are assumed to be small. For the comparison with the experiments the tangential strain in the middle of the joint and the mean value of the contact

Excerpt from ISBN 978-3-00-053387-7

pressure along the length of the joint are determined. The comparison of analytical and experimental results of the tangential strain shows that all analytical values are larger then the experimental ones. The deviation of the values is comparable for same thicknesses and gets larger the thicker the parts are. Also the calculated and measured assembly forces deviate most from each other for the thick combinations.

2. Methodolgy

The specimens from [2] are analysed with a numerical model and the results are discussed. These numerical results are compared with the experimental and analytical results from [2]. Based on this comparison it is evaluated which influence the mechanical phenomena have, that are neglected by the analytical approach from [1] and considered by the numerical model. A design parameter of the IFA, the thickness of the laminate layers, is investigated within a numerical parameter study.

3. Numerical Model

The numerical analysis of the test specimens is conducted with the commercial numerical software „Abaqus/CAE 6.14-2“ (Abaqus) from Dassault Systèmes. The assembled parts are modeled rotationally symmetric taking into account the measured geometry of each specimen. The inner diameter of the CFRP shaft is modeled with the same value than the outer diameter of the steel hub. The interference is defined during the contact definition. The CFRP shaft is modeled as a cylinder with half the length of the test specimen. For the 90°-layers a partition is defined and the ±30°-layers are subpartitioned to discretise these layers with a $(+30/-30)_8$-layup. At both ends of the contact area a part is cut out of steel hub and CFRP shaft and replaced by an independent part to enable a more detailed meshing of this region. Experimentally determined material parameters for the material given in [2] are used and adapted to the fibre volume contents of the ±30°- and 90°-layers of each test specimen with micromechanical formulas. Quadratic axisymmetric elements with reduced integration and included twist (CGAX8R in Abaqus) are used. Each partition of the ±30°-layers is meshed with one element. The global element length for steel hub and CFRP shaft is 2mm and a local length of 0,5mm is used for the contact area. The additional parts at the end of the contact area are meshed with elements of length 0,1mm. In total approximately 4000 elements are used for the whole model. Reference points at the ends of steel hub and CFRP shaft are coupled with the corresponding front surfaces in all degrees of freedom except the radial. The additional parts are tied to the steel hub or the CFRP shaft. The contact between the hub and the shaft is defined as frictionless in tangential direction. A surface-to-surface contact is defined, whereas the steel hub and its additional parts act as master surfaces. The interference is defined in the contact definition and is applied during the calculation. The two reference points are fully fixed. The described model is depicted in Figure 2. The calculation of the model is done in an implicit, geometrically nonlinear analysis. The tangential strain on the outer surface of the CFRP shaft as well as the contact pressure are determined along certain paths (see Figure 2). Within further data reduction the value of the tangential strain in the middle of the joint and the mean value $p_{c,m}$ of the contact pressure along the length of the joint are determined.

Excerpt from ISBN 978-3-00-053387-7

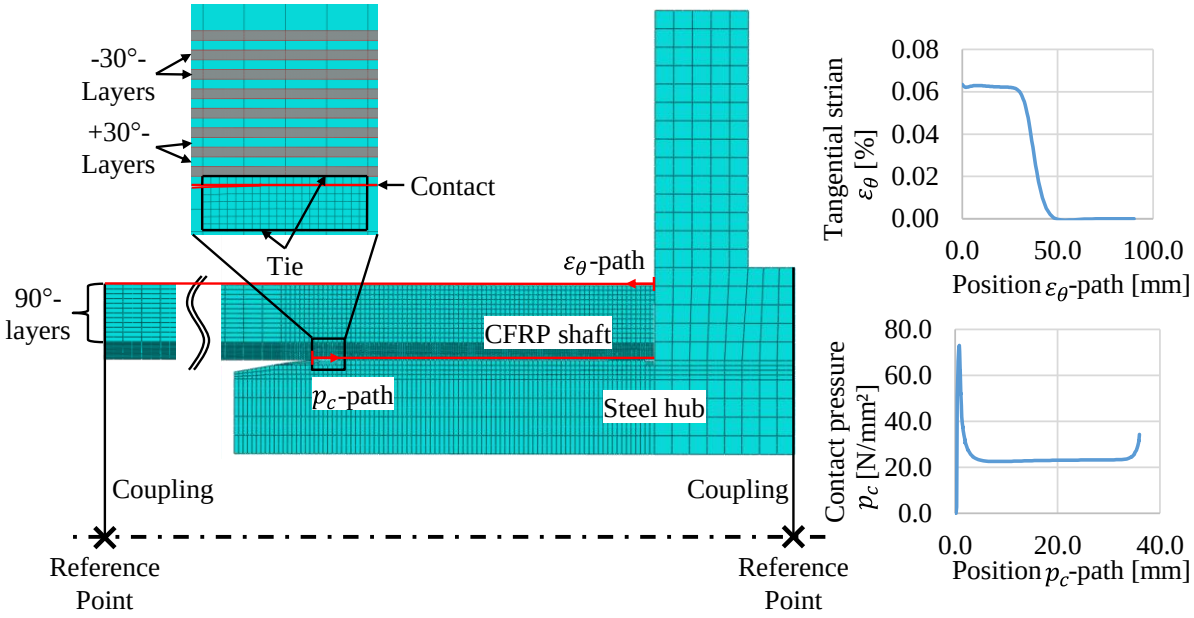

Figure 2. Meshed model of test specimen with definition of couplings, contact, ties, layup and paths for results

4. Numerical Simulation of Test Specimens

The specimens described in [2] have been analysed with the numerical model described in chapter 3. The mean values and standard deviations of $p_{c,m}$ are shown in Figure 3. The standard deviation results from the consideration of the measured geometry and material properties of each test specimen.

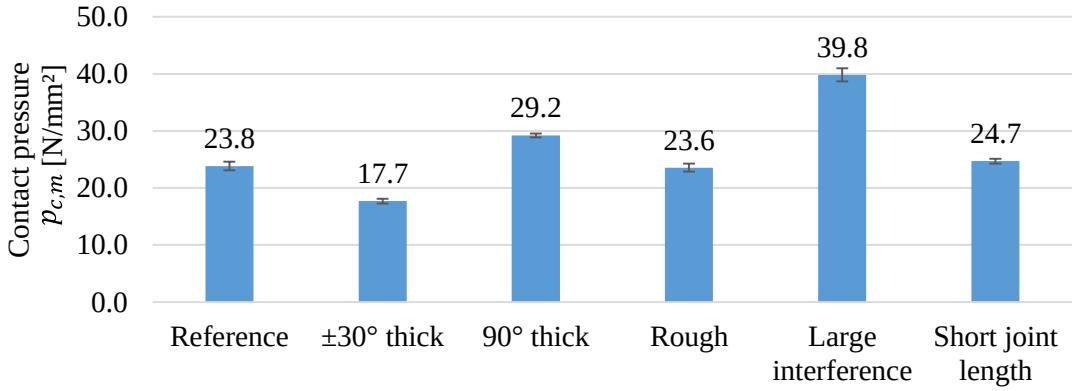

Figure 3. Mean values and standard deviations of the averaged contact pressure $p_{c,m}$

Compared to combination "Reference" $p_{c,m}$ decreases for combination "±30° thick". Increasing $t_{90°}$ less than proportionally increases $p_{c,m}$. Both these circumstances accord with the experimental results stated in [2] and show the great influence of the laminate layup. A detailed investigation within a parameter study and possible explanations are given in chapter 5. $p_{c,m}$ increases proportionally with the interference which shows the direct influence of this quantity and correlates with the results from

Excerpt from ISBN 978-3-00-053387-7

[2]. As the contact pressure has peaks at the ends of the contact area (see Figure 2) the slightly higher value of $p_{c,m}$ for combination "Short joint length" is plausible.

For the comparison with the experimental and analytical results the following values are used. The relative deviation $\Delta\varepsilon_\theta$ from calculated to measured tangential strain is calculated according to [2]. An effective coefficient of friction μ_{eff} (defined in [2]) is determined with the calculated contact pressure, the contact area and the measured assembly forces from [2]. The comparison of $\Delta\varepsilon_\theta$ for analytical (from [2]) and numerical values is depicted in Figure 4.

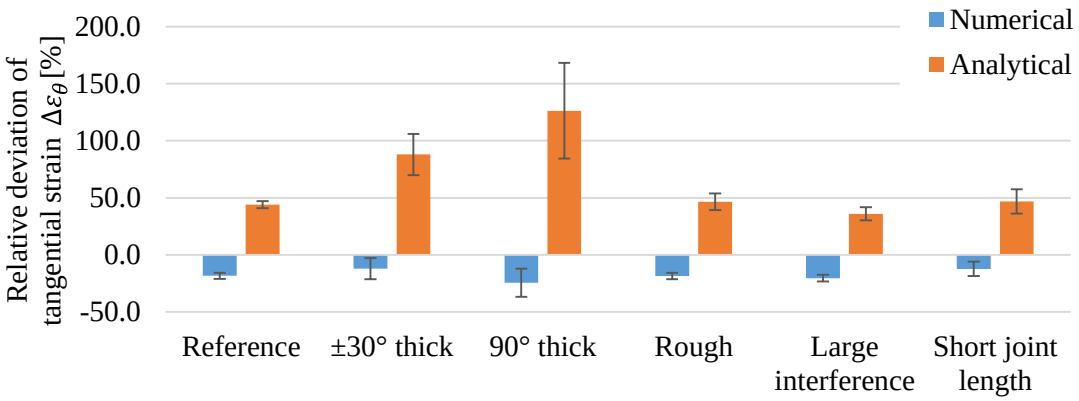

Figure 4. Relative deviation $\Delta\varepsilon_\theta$ from measured tangential strain for numerical and analytical values

For all combinations the relative deviation $\Delta\varepsilon_\theta$ of the tangential strain is positive for the analytical results and negative for the numerical results. The absolute values of $\Delta\varepsilon_\theta$ for the numerical results are smaller than for the analytical results. The analytical results show a strong dependency from the thickness of the test specimens. All these circumstances can be explained by the fact that the analytical approach neglects the radial deformation of the test specimens. The tangential strain is thus overestimated resulting in positive values $\Delta\varepsilon_\theta$, which increase for increasing thickness of the parts. The numerical model takes a radial deformation into account which results in smaller values of $\Delta\varepsilon_\theta$ and no tendency concerning the thickness of the parts.

The comparison of μ_{eff} for numerical and analytical values is shown in Figure 5.

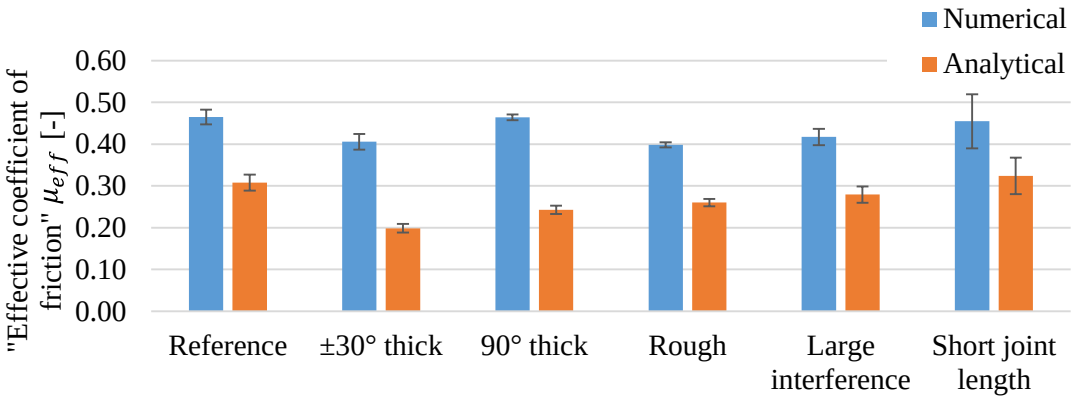

Figure 5. Comparison of μ_{eff} for numerical and analytical values

Excerpt from ISBN 978-3-00-053387-7

For all combinations μ_{eff} based on the numerical calculations is larger than the analytical ones. The numerical values of μ_{eff} vary in a smaller range and no dependency from the thickness of the parts can be seen. As mentioned before the analytical approach overestimates the tangential strain and thus also the contact pressure. By taking this deformation into account the numerical contact pressures are smaller and the values of μ_{eff} are larger than the corresponding analytical ones. Due to this the accuracy of the results also does not depend on the thickness of the parts. The relative deviation of the numerical values μ_{eff} from the value of combination "Reference" is largest for combination "Rough". A possible explanation are the different surface properties of the steel hub and thus different frictional conditions compared to the other combinations, in which all surfaces are manufactured the same way.

The following conclusions can be drawn from the conducted studies. The numerical values of $\Delta\varepsilon_\theta$ are smaller and μ_{eff} varies less than the analytical values. Furthermore both values show no dependency from the thickness of the parts for the numerical calculations in contrast to the analytical ones. The numerical model takes into account the radial deformation of the parts and the postion of each laminate layer. How strong the consideration of each of these effects influences the differences to the analytical results must be investigated in further studies. Concerning the application of the numerical model the following can be stated. As the numerical μ_{eff} varies less than the analytical values the assembly force for IFAs with same surface properties can be determined with more accuracy independent from the thickness of the parts by knowing μ_{eff} for this specific surface properties.

5. Investigation of the Influence of the Thickness of the Inner and Outer Layers

The experiments in [2] and the calculations in chapter 4 have shown that $F_{a,exp.}$ and $p_{c,m}$ decrease for an increase of $t_{\pm 30°}$ and increase for an increase of $t_{90°}$. The effect of increasing $t_{90°}$ gets smaller the thicker the parts are. In this chapter the influence of varying the thickness t_{BL} of the balanced layup and $t_{90°}$ is investigated for the laminate layout of the test specimens within a parameter study. The dependencies on the angle α_{BL} of the balanced laminate and the scale of the parts are also investigated.

The applied numerical model is comparable to the one described in chapter 3 except for the following deviations. Steel hub and CFRP shaft are cylinders with a length of 55mm and 100mm respectively, overlapping on a length of 35mm. The ±30°-layers of the CFRP shaft are subpartitioned to discretise these layers with a $(+30°/-30°)_2$ layup. The material properties of the material mentioned in [2] are adapted to a constant fibre volume content of 50% with micromechanical formulas. The ±30°-layers are meshed with one element per partition and the 90°-layers are meshed with 4 elements across the thickness. The total number of elements is 800 for the CFRP shaft and 550 for the steel hub. The coupling between reference points and corresponding front surface applies to all degress of freedom. The reference points themselves are fixed in axial direction. The step is implicit and geometrically linear. The determined result is the contact pressure p_{cM} in the middle of the joint.

Within the parameter studies the influence of increasing t_{BL} is investigated by keeping $t_{90°}$ constant and gradually increasing t_{BL}. The investigations for $t_{90°}$ are done the other way round. Both investigations are conducted for different values of the angle α_{BL} to evaluate its influence on the increase of the wall thickness. In Table 2 the values of the varied parameters are given, which are investigated in a full factorial parameter study. The influence of the scale of the parts is investigated for representative parameters (underlined values in Table 2). The inner diameter of the CFRP shaft, the length of the joint, the thicknesses t_{BL} and $t_{90°}$, the interference between the parts, the thickness of the steel hub and the free lengths of the parts are scaled with two different scale factors Sc.

Excerpt from ISBN 978-3-00-053387-7

Table 2. Overview of varied parameters (underlined values varied within investigation of scaled parts)

Designation [Unit]	Values								
t_{BL} [mm]	0.25	0.50	1.00	1.50	2.00	3.00	4.50	6.00	9.00
$t_{90°}$ [mm]	0.25	0.50	1.00	1.50	2.00	3.00	4.50		
α_{BL} [±°]	30	45	60						
Scale factor Sc [-]	0.5	2							

The results for the variation of $t_{90°}$ for different values of t_{BL} and α_{BL} are shown in Figure 6.

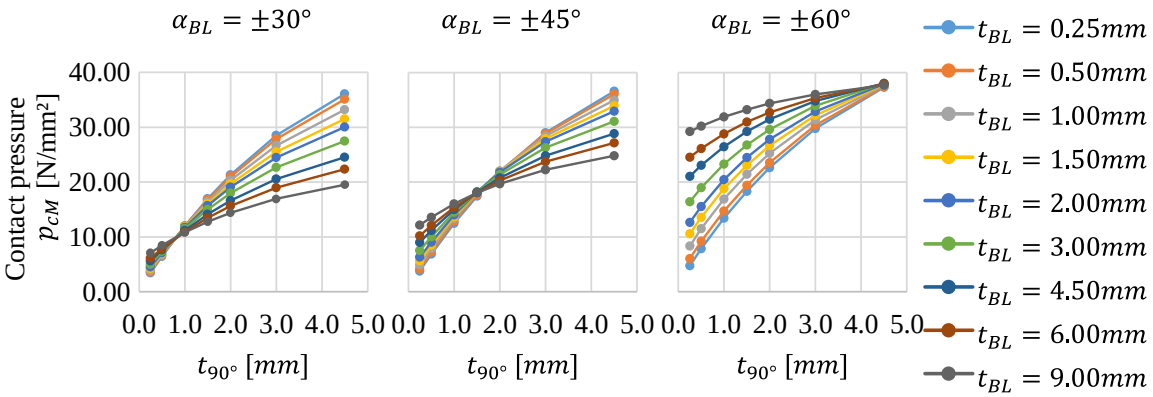

Figure 6. Variation of $t_{90°}$ for different values of t_{BL} and α_{BL}

An increase of $t_{90°}$ increases p_{cM} for all thicknesses t_{BL} and angles α_{BL}. This is plausible as the additional layers stiffen the CFRP shaft. The secant gradients of the curves get smaller the higher $t_{90°}$ and t_{BL} get. Both is plausible as additional layers are strained less the thicker the parts are due to the decrease of the tangential strain with the radius of the part. All curves of one graph intersect at nearly one point for which p_{cM} is almost independent of t_{BL}. This point varies for different values of α_{BL}.

The results for the variation of t_{BL} for different values of $t_{90°}$ and α_{BL} are shown in Figure 7.

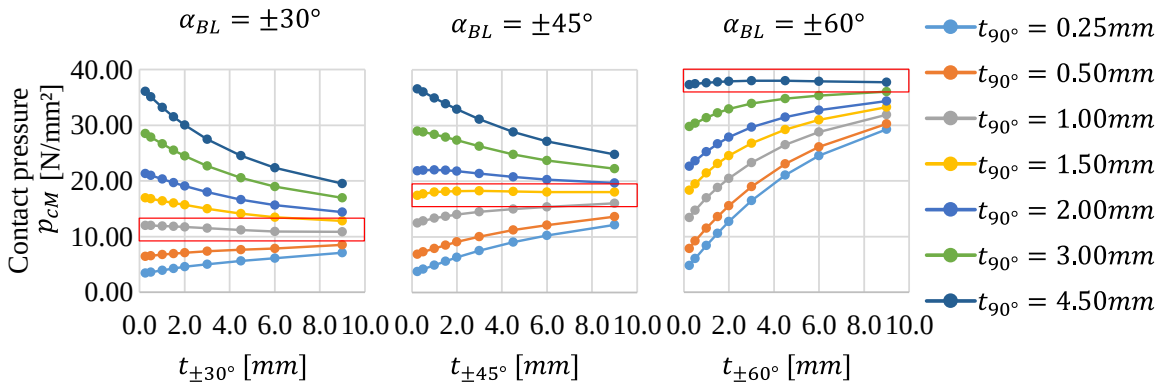

Figure 7. Variation of t_{BL} for different values of $t_{90°}$ and α_{BL} (critical thicknesses $t_{crit.}$ marked red)

Excerpt from ISBN 978-3-00-053387-7

For all investigated angles α_{BL} a thickness $t_{90°}$ exists for which p_{cM} is almost constant despite variation of the thickness t_{BL}. In the following these thicknesses are called "critical thickness" $t_{crit.}$, which are marked in Figure 7 and represented by the intersection points in Figure 6. For values of $t_{90°}$ smaller than $t_{crit.}$ the contact pressure p_{cM} increases with increasing thickness t_{BL}. In most cases this increase gets smaller the bigger $t_{90°}$ and t_{BL} are. For values of $t_{90°}$ bigger than $t_{crit.}$ the contact pressure p_{cM} decreases in most cases with increasing thickness t_{BL}. This decrease gets bigger the bigger $t_{90°}$ is and smaller the bigger t_{BL} is. Deviations from these dependencies appear for values of $t_{90°}$ close to $t_{crit.}$ and small values of t_{BL}. The values of $t_{crit.}$ get smaller the smaller α_{BL} is.

The scaled geometry's results for variation of $t_{\pm 30°}$ for different values of $t_{90°}$ are shown in Figure 8.

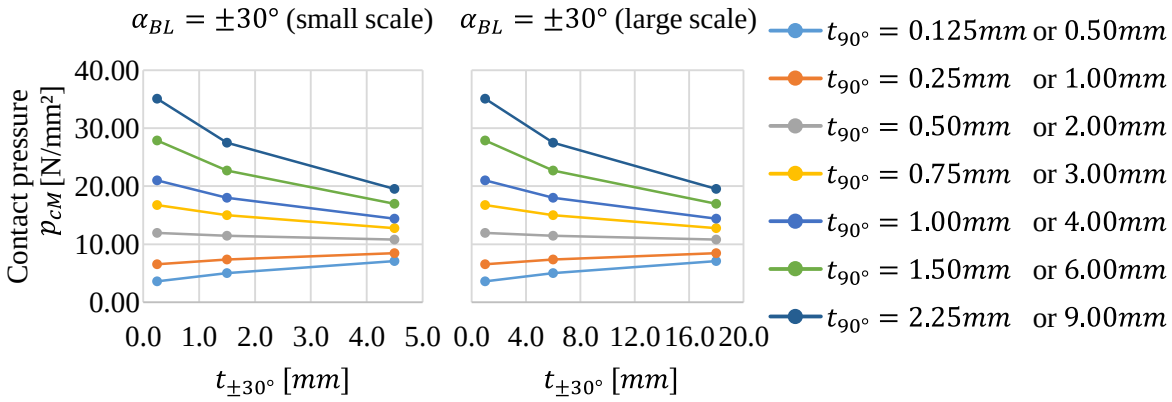

Figure 8. Variation of $t_{\pm 30°}$ for different values of $t_{90°}$ and different scales of the parts

For the different scales of the parts p_{cM} is identical. The values for $t_{crit.}$ are therefor also scaled with the scaling factor Sc.

The following conclusions can be drawn from the conducted studies. The larger the thickness of the laminate is the smaller the influence on p_{cM} of adding additional 90°-layers on the outer surface gets. In terms of weight this is even more pronounced as it increases with the square of the thickness, which means that to increase the contact pressure by a certain amount more weight needs to be added the thicker the parts are. For $t_{90°}$ larger than a critical thickness an increase of t_{BL} decreases p_{cM}. If possible the additional balanced laminate layers should be positioned on the outer surface in this case. Generally 90°-layers should be postioned close to the contact area to achieve high values of p_{cM}. The critical thickness of 90°-layers varies with the angle of the balanced laminate and can be scaled with the corresponding scaling factor for scaled parts. Further dependencies of the critical thickness must be investigated in upcoming studies.

6. Outlook

Within the experimental studies and analytical calculations in [2] as well as the comparison with the numerical calculations in this paper several design parameters and mechanical or tribological phenomena have been hypothesized. These parameters and phenomena have to be investigated to corroborate the hypotheses. The investigations are done by numerical or experimental studies like in chapter 5 to prove the existence of the phenomena and evaluate and compare their influence.

Excerpt from ISBN 978-3-00-053387-7

References

[1] T. Fischer. *Der Pressverband als torsionsbelastete Krafteinleitung in Faser-Kunststoff-Verbund-Wellen.* Schriftenreihe Konstruktiver Leichtbau mit Faser-Kunststoff-Verbunden, Shaker Verlag, Aachen, 2005.

[2] P. Fahr and R. Hinterhölzl. Evaluation of an analytical analysis method for interference fit assemblies focusing on thick-walled parts based on experimental data. *Proceedings of the 20th International Conference on Composite Materials ICCM-20, Copenhagen, Denmark,* July 19-24 2015.

Excerpt from ISBN 978-3-00-053387-7